

This report shows the possibilities of clock synchronization using time signals transmitted at low frequencies. The study was made by observing pulses emitted by HBC (75 kHz) in Switzerland and by WWVB (60 kHz) in the United States.

The results show that the low frequencies are preferable to the very low frequencies. Measurements show that by carefully selecting a point on the decay curve of the pulse it is possible at distances from 100 to 1000 kilometers to obtain time measurements with an accuracy of ± 40 microseconds.

A comparison of the theoretical and experimental results permits the study of propagation conditions and, further, shows the desirability of transmitting seconds pulses with fixed envelope shape.

Reprinted from FREQUENCY,
Vol. 6, No. 9, pp 13-21
(September 1968),

RECEPTION OF LOW FREQUENCY TIME SIGNALS

DAVID H. ANDREWS

P. E., Electronics Consultant*

C. CHASLAIN, J. DePRINS

University of Brussels, Brussels, Belgium

I. INTRODUCTION

For several years the phases of VLF and LF carriers of standard frequency transmitters have been monitored to compare atomic clocks.^{1,2,3}

The 24-hour phase stability is excellent and allows frequency calibrations to be made with an accuracy approaching 1×10^{-11} . It is well known that over a 24-hour period diurnal effects occur due to propagation variations. Fig. 1 shows this effect over a 24-hour period relatively small for LF at medium distances.

While this method is adequate for frequency com-

parisons of atomic clocks, it does not suffice for clock synchronization (epoch setting). Presently, the most accurate technique requires carrying portable atomic clocks between the laboratories to be synchronized. No matter what the accuracies of the various clocks may be, periodic synchronization must be provided. Actually the observed frequency deviation of 3×10^{-12} between cesium controlled oscillators amounts to a timing error of about 100T microseconds, where T, given in years, is the interval between synchronizations.

Another approach is to effect synchronization by means of HF time signals (3-30 MHz). Such signals are usually provided by carrier modulation for a short interval at a frequency near 1 kHz (Fig. 2). Epoch is obtained by observing the time of a 'significant point, say the first maximum of the modulation pulse.

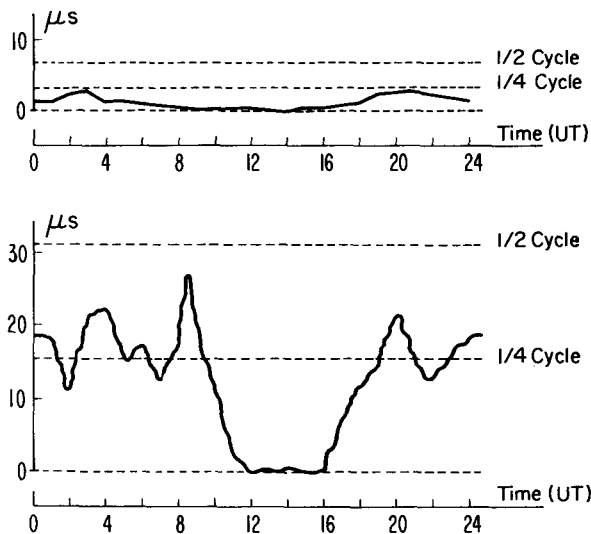


Figure 1 — (Top) Diurnal phase variation of HBC;
(Bottom) Diurnal phase variation of GBR.

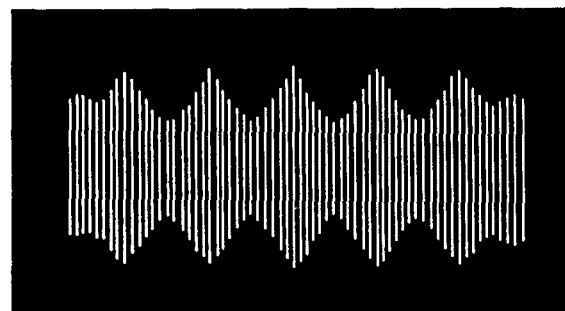


Figure 2 — High frequency time signals.

* This work was performed before Mr. Andrews' retirement from the National Bureau of Standards, Boulder, Colo.

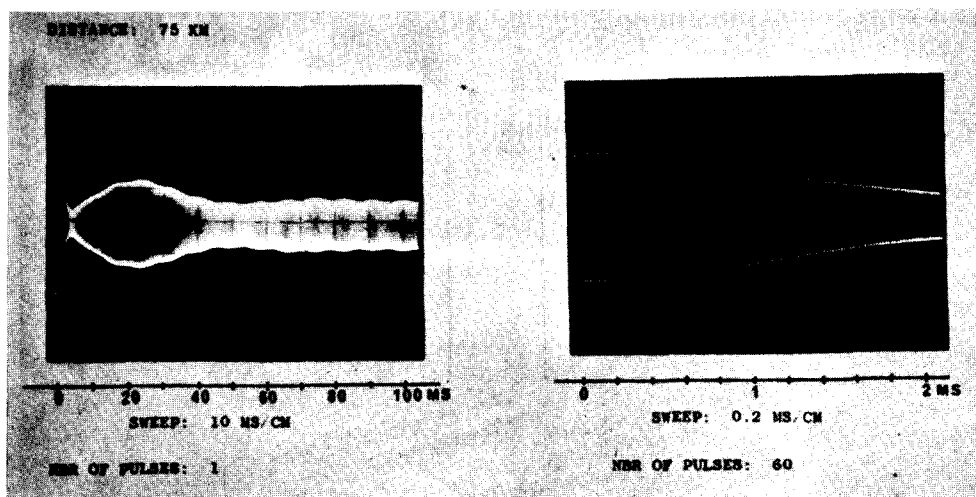


Photo 1 — Boulder, 8 April, 1967, 8H (U.T.)

Clearly, for high frequencies, the shape of the received modulation signal depends neither upon the antenna characteristics, nor, in general, upon the receiver characteristics. But, propagation conditions change the effective path length, and variations in arrival time of the pulse may reach hundreds of microseconds.

The daily phase stability at LF (Fig. 1), indicates that a single mode of propagation is dominant at 500 km. It would appear, then, that low frequencies are suitable for transmitting time signals. The low frequencies, however, cannot utilize modulation like that used at HF because the high antenna "Q" strongly affects the desired modulation shape. The receiver system will also degrade the modulation envelope.

The system studied utilizes carrier modulation by a square pulse, which undergoes some degradation by the transmitter tuning system. The antenna tuning and its "Q" depend upon weather conditions so that the radiated pulse varies in the course of time.

The pulse is further distorted by the receiver. Photo 1, made of WWVB in Boulder, shows a typical envelope. The length of the decay time (about 2 ms) with respect to the desired accuracy makes it difficult to define a suitable "timing" point.

Ideally one could find the exact analytical expression for the complete envelope and by comparison with experimental results define the arrival time. Such an approach is not feasible with present transmitting conditions.

The purpose of this work has been to select and measure a suitable "timing" point. A precision of ± 40 microseconds is assured by the system here proposed. In Brussels, for example, this method has provided time synchronization with this accuracy, and frequency measurements on a yearly basis were in error by less than 7 parts in 10^{12} . These results were obtained using

a quartz clock. The economic appeal of this method is strong since the synchronizing equipment can be set up for a few hundred dollars and gives results comparable to those obtained using atomic clocks costing from \$10,000.00 to \$20,000.00.

Improvements in emission, particularly in the transmitted envelope shape, coupled with synchronization between transmissions at LF and VLF would permit synchronization to the order of a microsecond, if the path delay is known.

In conclusion, we note that this accuracy is actually attained, in a restricted area (East Coast U.S.A.) with the Loran-C navigation system using a low frequency.^{4,5,6} It would be very interesting, in view of the Loran-C results and some of the aforesaid con-

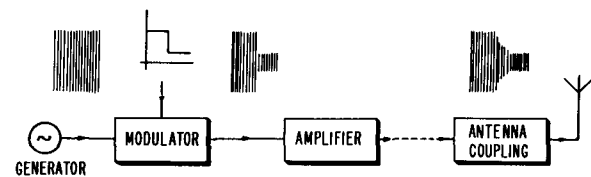


Figure 3. — Simplified block diagram of a transmitter.

siderations, to build a transmitter solely devoted to synchronization and which does not have the drawbacks of Loran-C, namely, difficulty in pulse identification and pulse repetition rate, and inadequate coverage except in Eastern United States.

II. EMISSION OF TIME SIGNALS

A transmitter is shown schematically in Fig. 3, including the waveshapes resulting in the final radiated signal.

At low power, the carrier is amplitude modulated by a rectangular pulse. The resulting signal is then amplified to the required power, about 30 kilowatts, and coupled through a transmission line to a resonant antenna.

Characteristics of the transmitters studied are given in Table I.

TABLE I
Transmitter

	HBG	WWVB
Location * [7]	Prangins (Switzerland) 46°N 6°N	Fort Collins (USA) 40°40.5'N 105° 2.5'E
Frequency	75 kHz	60 kHz
Power	20 kW	13 kW
Carrier frequency	AT (1)	AT (1)
Phase control	No	Yes
Time Signal System	UTC (2)	SAT (3)
Modulation	Carrier cut-off	WWVB Time Code
Characteristics	each second (4)	[11]

(1) AT = atomic time [7]

(2) UTC = coordinated universal time [7]

(3) UTC is approximated by AT with 200-ms steps

(4) The minute is identified by two successive 100-ms carrier cut-offs separated by 100 ms.

* Numbers in brackets refer to references.

III. THEORETICAL ENVELOPE SHAPE

While the low power driving signal is basically a square wave, this is not true for the emitted signal, nor for the received signal. The modulated signal is distorted both by the electronic circuits in the transmitter and receiver and also by propagation of the electromagnetic waves through the ionosphere.

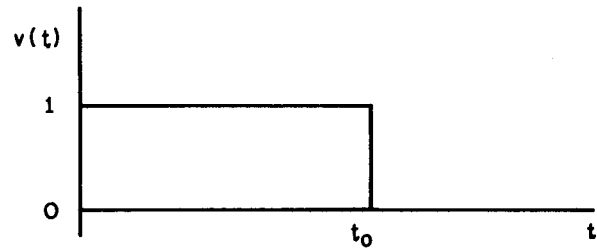


Figure 4.

To calculate the envelope shape it is hardly possible to consider in detail all the electronic circuits of the transmitter and receiver. The following simplifying hypotheses are made:

- The transmitter and receiver are linear amplifiers with tuned RLC circuits.
- The envelope shape remains unchanged for the propagation mode considered.

The most important results are contained in the remainder of the report. Details of the calculations involving Laplace transforms may be found in Chaslain's paper.⁸

III-1. Response of circuits tuned to different frequencies to a single pulse

The driving modulation signal $v(t)$ is shown in Fig. 4, where

$$v(t) = u(t) = \begin{cases} 1 & 0 < t < t_0 \\ 0 & t < 0, t > t_0 \end{cases}$$

The theoretical response for three circuits in series is given by:

$$i_3(t) = \frac{\beta}{L_1 L_2 L_3} \left\{ \sum_{i=1}^3 \frac{\rho_i}{\eta_i c_i} e^{-\mu_i t} \sin(\eta_i t + \varphi_i) - \sum_{i=1}^3 \frac{\rho_i}{\eta_i c_i} e^{-\mu_i (t-t_0)} \sin[\eta_i (t-t_0) + \varphi_i] u(t-t_0) \right\} \quad \{1\}$$

where ω_i , L_i , R_i refer to the frequency, inductance, and resistance of the i th circuit, and where

$$\rho_i = \sqrt{[(\omega_i^2 + 2\mu_i^2)\delta_i + 2\mu_i\eta_i\gamma_i]^2 + [\delta_i(\omega_i^2 + 2\mu_i^2) - 2\mu_i\eta_i\delta_i]^2}$$

$$c_i = (A_{ij}^2 + B_{ij}^2)(A_{ik}^2 + B_{ik}^2)(1 - \epsilon_{jk})$$

$$\epsilon_{jk} = \begin{cases} 1, & j = k \\ 0, & j \neq k \end{cases}$$

$$\mu_i = \frac{\omega_i}{2Q_i}; \quad Q_i = \frac{\omega_i L_i}{R_i}; \quad \eta_i^2 = \omega_i^2 - \mu_i^2$$

$$A_{ij} = (\omega_j^2 - \omega_i^2) + 2\mu_i(\mu_i - \mu_j)$$

$$B_{ij} = 2\eta_i(\mu_i - \mu_j)$$

$$\delta_i = (A_{ij}A_{ik} - B_{ij}B_{ik})(1 - \epsilon_{jk})$$

$$\gamma_i = A_{ij}B_{ik} + A_{ik}B_{ij}(1 - \epsilon_{jk})$$

$$tg\varphi_i = \frac{\gamma_i(\omega_i^2 + 2\mu_i^2) - 2\mu_i\eta_i\delta_i}{\delta_i(\omega_i^2 + 2\mu_i^2) + 2\mu_i\eta_i\gamma_i}$$

III-2. Study of the effects on a carrier amplitude modulated with a square wave.

The signal to be transmitted is shown in Figure 5 and is given by:

$$v(t) = A \sin \omega t - c \sin \omega t u(t - t_0),$$

where u is the previously defined modulation signal.

For n circuits in series tuned to the same frequency, their behavior, during carrier suppression, is given by:

$$i_n(t) = \frac{kA}{2^n \pi} \left\{ \frac{1}{L_1(t-t_0)} \left[\sin \omega t - \frac{c}{A} \left[\sin \omega t - \sum_{i=1}^n \frac{\omega}{\eta_i} \frac{e^{-\mu_i t}}{\prod_{\substack{j=1 \\ j \neq i}}^n \left(1 - \frac{\mu_j}{\mu_i}\right)} \right] u(t-t_0) \right] \right\} \quad \{2\}$$

with the symbols:

$$L_1(t-t_0) = \frac{1}{\omega} \left\{ \rho_i \sin [\eta_i(t-t_0) + \varphi_i] - \mu_i \sin \omega t_0 \sin \eta_i(t-t_0) \right\}$$

$$tg\varphi_i = \frac{\eta_i}{\omega} tg\omega t_0$$

$$\rho_i = \omega \sqrt{1 - \frac{1}{4Q_i^2} \sin^2 \omega t_0}$$

If the beginning of the pulse is synchronized with the carrier and if $4Q_i^2 \gg 1$, we get

$$i_n(t) = \frac{kA}{\omega^n} \left(\frac{Q_i}{L_1} \right) \left\{ 1 - \frac{c}{A} \left[1 - \sum_{i=1}^n \frac{e^{-\frac{\omega}{2Q_i} t}}{\prod_{\substack{j=1 \\ j \neq i}}^n \left(1 - \frac{Q_j}{Q_i}\right)} \right] u(t-t_0) \right\} \sin \omega t. \quad \{3\}$$

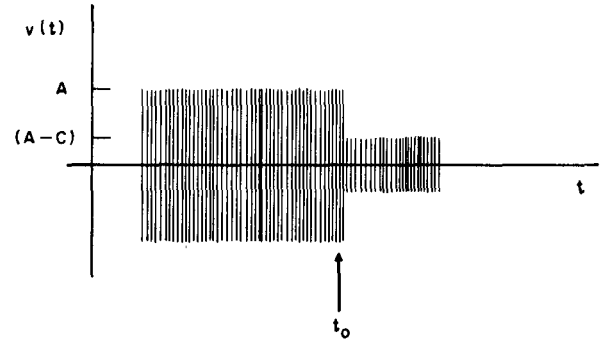


Figure 5.

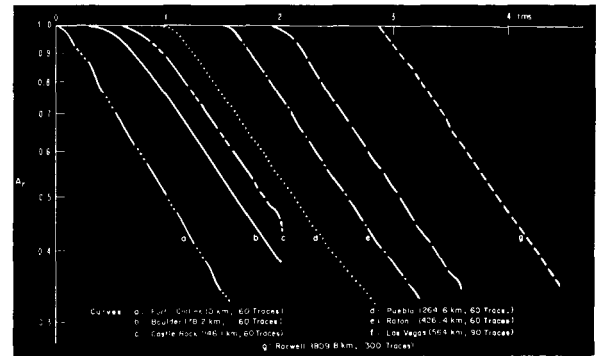


Figure 6. — Envelope shape versus distance between transmitter and receiver.

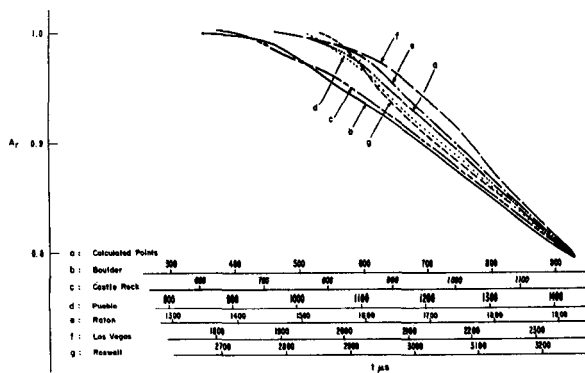


Figure 7. — Envelope shape versus distance between transmitter and receiver.

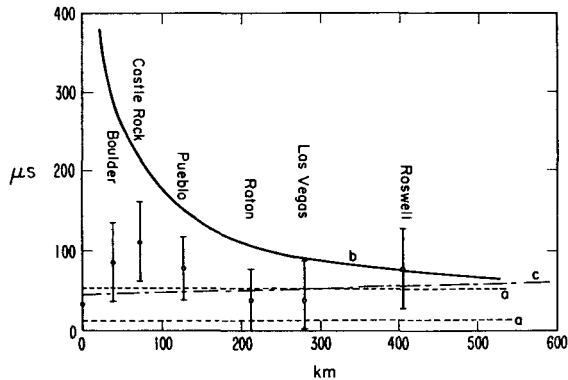


Figure 8. — Curve a: Ground wave. Curve b: Wave reflected once at an altitude of 70 km. Curve c: Linear regression curve.

III-3. Remarks.

1. In assuming a simplified model composed of two tuned circuits, one for the transmitter and the other for the receiver, we obtain a response curve which immediately shows several discrepancies. For instance, it is very reasonable for the "Q" of the transmitting antenna to vary by 10% due to atmospheric changes. In this case, for realistic conditions, time variations for fractional amplitudes between 0.5 and 1.0 are given in Figure 13.

This graph seems to show that it should be possible to synchronize at the beginning of the time pulse. But experimentally this cannot be done precisely due to the slow rate of change of amplitude at the beginning of the pulse. The amplitude decreases by 0.5% during the first 100 microseconds and only 3% during the first 200 microseconds.

2. The expression $\{2\}$ points out that the time tick must be locked to the carrier if distortion is to be avoided.

IV. ENVELOPE MEASUREMENTS

IV-1. Receivers.

Reception conditions for transmissions from HBG

and WWVB are different. Time pulses from HBG were received at Brussels, a distance of 506 km, under high noise level conditions, whereas time signals from WWVB were usually received at Boulder, a distance of 78.2 km, and at all times under low noise conditions. Two different receivers were constructed having the following characteristics shown in Table II.

TABLE II

		Receiver	
		Brussels [9]	U.S.A.
Frequency		75 kHz	60 kHz
Field Strength		$650 \pm 20 \mu\text{V/m}$	35 mV/m
Antenna	General Characteristics	Ferrite Tube Phillips 56.261.36/3 B	Tuned Loop Primary: 25 turns Secondary: 6 turns
	Resonant Impedance	23.5 k Ω	50 k Ω
	"Q"	50	22
Preamplifier	Gain	56 dB	39 dB
	Voltage Amplification	30	11
Receiver	Output Impedance	2.5 k Ω	0.5 k Ω
	Gain	46 dB	43 dB
	Voltage Amplification	1500	420
	"Q"	Variable between 100 and 300	22

IV-2. Measuring systems.

The first problem is to minimize the effects of short term random fluctuations due to propagation, of man-made noise, and of interference from transmitters with carrier or side-band frequencies near the useful signal. The observed signal-to-noise ratio usually lies between 5 and 20. Visual observation of the seconds pulses generally does not give an accuracy better than several hundred microseconds for time comparison.

The accuracy was improved by photographically superimposing many successive time pulses. It is clear that this technique requires the phase between the received signal and the local reference to remain constant during the integrating time. Thus a compromise between the signal-to-noise ratio and the desired accuracy was necessary.

Thus, the higher the receiver "Q" the better the signal-to-noise ratio, but the pulse rise-time increases and lowers the accuracy. This compromise has determined the "Q" of the receivers.

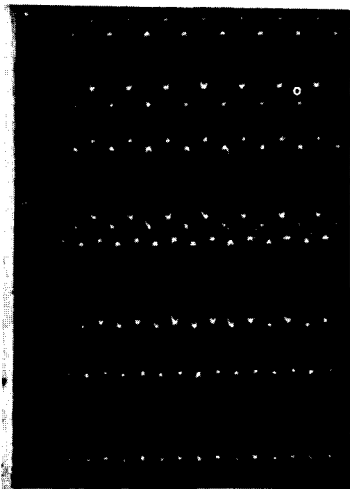


Photo 2 — Brussels, 19 June, 1967, 1605H (U.T.). Sweep: 10 $\mu\text{s}/\text{cm}$; number of pulses: 60.

At Brussels, the envelope of HBG was determined by measuring the amplitudes at selected points on the curve. This accomplished by photographically superimposing several cycles, selected with a variable delay line from a number of consecutive pulses.

For calibration purposes the maximum amplitude is also recorded on the photograph (Photo 2). The measurement precision of the relative value lies between 0.005 and 0.03.

In the United States, with a better signal-to-noise ratio, the entire envelope was recorded on a single photograph. The amplitude was measured to a precision of from 0.002 to 0.008.

Later in the report, Figure 15 shows the timing error versus an amplitude measurement error of 0.01. As might reasonably be expected, the function shows a minimum.

V. EXPERIMENTAL RESULTS

V-1. Study of transmission characteristics.

It was desirable to confirm the correspondence between the theoretical model and the radiated signal, for it would be useless to study the model if there was a substantial difference in the radiated signal.

Moreover, this approach allows the transmission characteristics to be considered as initial data.

For HBG, the proximity of other more powerful transmitters has, for now, prevented measurements on the antenna. On the other hand, complete measurements have been made for WWVB.

It was first noted that the emitted signal had a rather complex waveform. For the first 3 milliseconds, the decay was exponential, agreeing with the mathematical model. Then between 3 and 100 milliseconds an overshoot, followed by a damped oscillation, occurred which was probably attributable to the transmission line and antenna matching system. Hereafter the study is limited to the first period.

Measurements on the low-power driving signal show a small amplitude modulation ($\pm 2\%$) and a slight frequency modulation, and they also show that the time

required for the signal to reach the reduced level was in the order of 35 microseconds. In addition, a slight overshoot was observed. Despite these defects this signal can be satisfactorily represented by a square wave for mathematical analysis.

The antenna current was then investigated using an untuned loop coupled to the antenna ground lead, the signal from which was observed directly on an oscilloscope. The envelope of the signal agreed with the theoretical one except for a parasitic damped oscillation at 4 kHz with an amplitude of 0.02 and decay time of 310 microseconds.

The radiated signal in the immediate vicinity of the transmitting antenna was studied using the WWVB receiver and a 5 cm whip antenna. The envelope of the signal agreed with theory for a receiver having a "Q" of 22. The damped oscillation was quenched by the receiver filter.

A comparison of the two envelopes showed nonlinearities of the oscilloscope and receiver of less than 1% and 2%, respectively.

The measurements make possible an estimation of the parameters for the theoretical formulas using the least-squares method of fitting curves to the experimental data.¹⁰

The values obtained are shown below in Table III.

TABLE III

	From Antenna Current	By Receiver with 5 cm Whip Antenna
t_0	$27 \pm 20 \mu\text{s}$	$30 \pm 35 \mu\text{s}$
Q_1	205 ± 5	200 ± 5
A_r	0.90 ± 0.02	0.91 ± 0.02
Q_2	0	22 ± 3
σ_{adapt}	0.0065	0.0065
σ_{exp}	0.003	0.003

The relationship used was formula {3} with $n = 2$, σ_{adapt} = standard deviation, σ_{exp} = standard deviation, all estimated from measurement conditions.

These measurements emphasize the agreement between observed and predicted envelope shape. They also show whether the observed anomalies are liable to affect the overall accuracy of the measurements.

V-2. Study of receiving conditions.

Since the transmission data for HBG were not known accurately, better results were obtained from WWVB as received at Boulder, 78.2 km distance.

Early measurements revealed that the waveshape received in Boulder varied with time. This was in disagreement with the theory, particularly for amplitudes between 1.0 and 0.8. (Deviations are as much as 0.05 with a measurement precision of 0.003.)

These data show that it is necessary to consider the received signal as a composite of several propagation modes. On the other hand, the carrier phase stability is such that, during the day, the same propagation mode prevails.

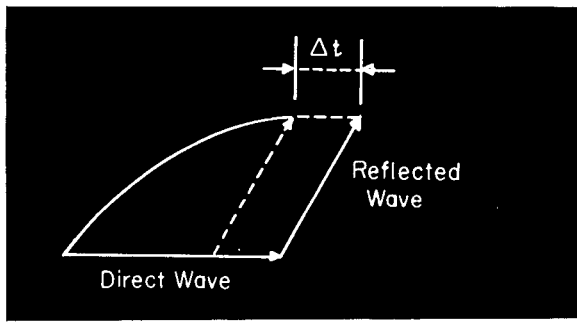


Figure 9. — Vector diagrams for envelope shape.

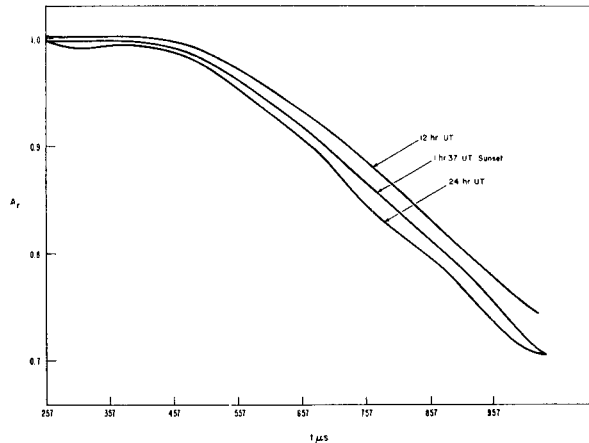


Figure 10. — Variations of envelope shape for a 24-hour period at Boulder.

The hypothesis is then made that propagation occurs with two modes, one of which predominates, the other possibly being present. This hypothesis was then tested to see if it was in agreement with the observations and, if so, to determine the dominant mode and the occurrence of the secondary mode.

In general, one expects for low frequencies that the ground wave is dominant for distances less than 1000 km.

To establish this hypothesis, the envelope of WWVB was measured as a function of distance between the transmitter and receiver for distances from 0 to 800 km. Figure 6 shows the results obtained using the low-level clock pulse as the time of origin. A careful study of these results shows coincident curves for fractional amplitudes less than 0.8, with a standard deviation for the fractional amplitude of 0.003 which corresponds exactly with the measurement error.

Note, however, that Figure 7 shows significant differences when the relative amplitudes lie between 0.8 and 1.0. It is quite evident that the shapes of the envelopes at Boulder and Castle Rock differ markedly from the theoretical single wave shape. These shapes, and also the others, support the presence of a second hop. The pulse beginning can be determined to an accuracy of ± 50 microseconds. Figure 8 gives, with the same time scale as the preceding figures, the arrival time of the

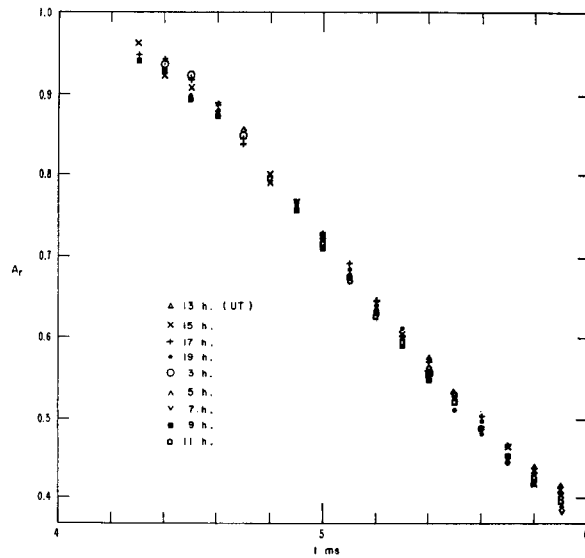


Figure 11. — Variations of envelope shape for a 24-hour period at Brussels.

commencement of the time pulse, from which the propagation time for a direct wave traveling at the speed of light may be deduced. These data demonstrate without doubt that (at least to 500 km) ground wave propagation exists. The propagation velocity is $(2.985 \pm 0.015) 10^8$ meters per second.

It is possible to consider that the envelope shape is derived from a dominant ground wave combined with a delayed skywave. It also seems reasonable to assume that the skywave propagates by a single hop. Under these conditions the resultant envelope shape is derived by adding the envelope of two carriers having the previously determined theoretical shape. To perform these calculations three new factors are introduced:

- a. Phase difference between the carriers.
- b. Skywave time delay (including phase change or reflection).
- c. Relative amplitude of skywave.

Using a computer, a set of tables was prepared showing the resultant envelope shapes as a function of these parameters.

Propagation conditions over a 24-hour period were observed both at Boulder and Brussels.

At Boulder, 78.2 km from WWVB, the additional time delay for the skywave is about 260 microseconds assuming the ionospheric reflecting layer is around 70 km high. Results obtained in Boulder are shown in Figure 10. Groundwave propagation accounts for 50% of the observed envelope shapes. Comparing the other envelopes with the calculated tables shows that the skywave varies between 0 and 30% of groundwave amplitude. From this, a phase variation of about 1 microsecond would be expected, which was indeed observed in Boulder. Finally, during the period from 16 hours to 24 hours UT, or from sunrise to several hours before

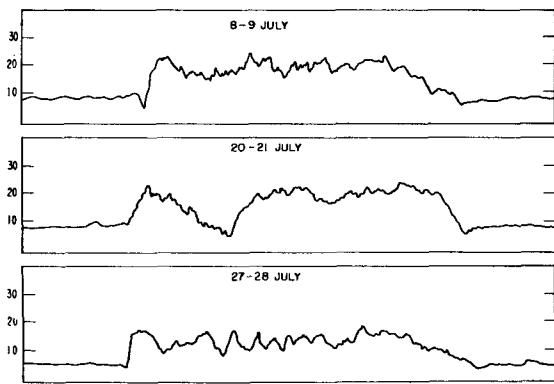


Figure 12. — Recording of field strength of HBG at Brussels.

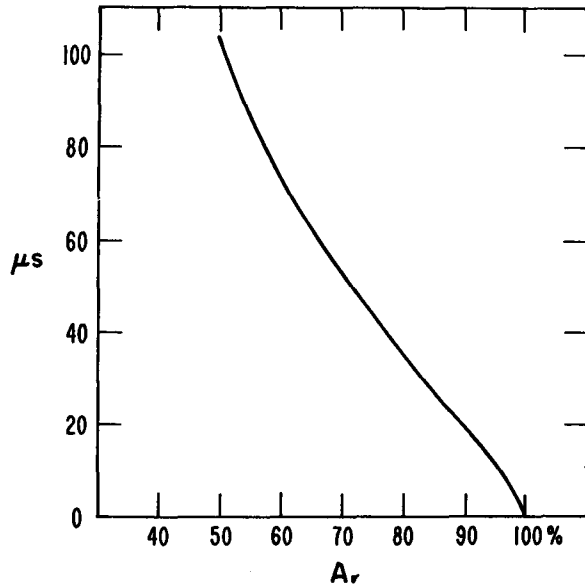


Figure 13. — Timing error due to a 10% variation in "Q" of the transmitting antenna.

sunset, the envelope has the shape predicted for a single mode of propagation.

In Brussels, 506 km from HBG, the additional time delay for the skywave is on the order of 70 microseconds, which fortunately reduces the influence of propagation on the envelope shape. Figure 11 shows the effect of superimposing nine curves taken at regular intervals throughout a 24-hour period. Here also the results are consistent with groundwave propagation during the day and with a nighttime skywave having a relative amplitude of 0 to 30% of its groundwave.

Interesting additional information is seen in the total received amplitude. Figure 12 shows several consecutive graphs. These are not easy to interpret since the amplitude is strongly dependent on the phase difference between the direct and reflected waves. Some points, however, are quite clear:

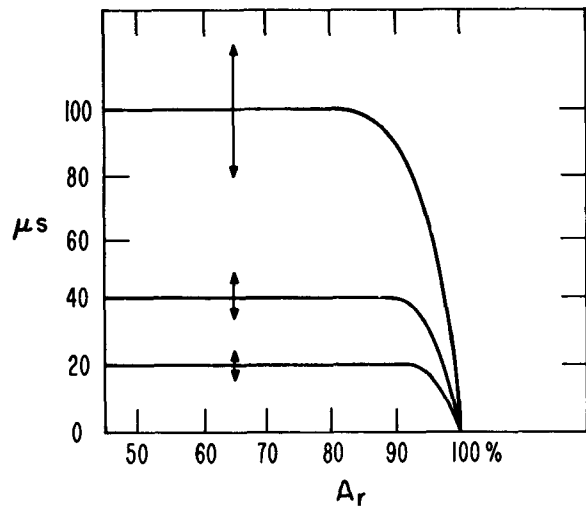


Figure 14. — Timing error due to a change of propagation from 100% ground-wave to 60% ground-wave and 40% sky-wave reflected at an altitude of 70 km.

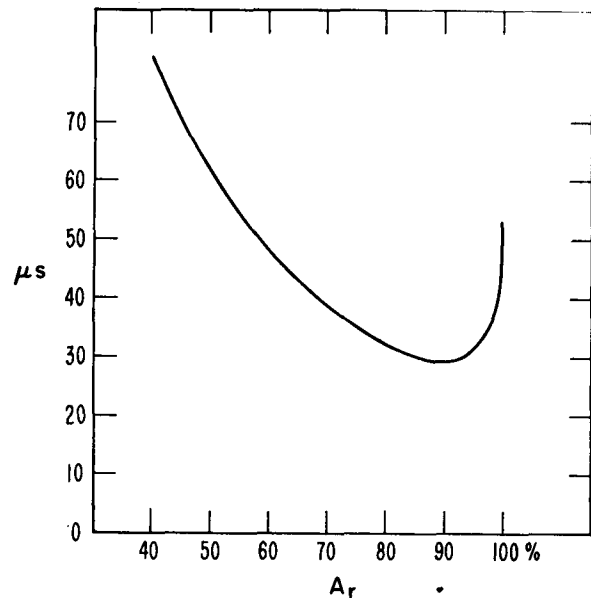


Figure 15. — Timing error due to an amplitude error of 0.01.

- a. Daytime propagation is very stable and composed essentially of the groundwave.
- b. From shortly before sunset until sunrise skywave also exists.
- c. An abrupt change occurs at sunrise.

VI. CONCLUSIONS

The experimental data point out the complexity of the mathematical treatment for the time signal envelope. Unambiguous determination of both the propagation parameters and the transmission parameters is not possible by simultaneous measurements at the receiver.

The first result of this study is to show the desirability of transmitting a pulse with constant, precisely known shape. When this is done, assuming known receiver characteristics, only propagation conditions remain to be determined.

Otherwise, given certain conditions of transmission and reception, the determination of propagation conditions will be facilitated if the "Q's" of the transmitter and receiver are low. This implies powerful transmissions from a low "Q" antenna. The Loran-C transmissions are of this type and permit excellent synchronization.

If one uses time signals as presently transmitted at low frequencies, the time of arrival can be determined from a selected point on the pulse envelope. The timing error in using this method is a function of the amplitude chosen and the following phenomena:

- a. Changes in pulse shape due to variations in the transmitting antenna (Figure 13).
- b. Variable propagation conditions (Figure 14).
- c. Errors in measuring the amplitude of the received pulse envelope (Figure 15).

The overall error (Figure 16) has a minimum depending on the relative magnitudes of the three types of errors. Generally a minimum overall error prevails when the amplitude point is selected between 0.9 and 0.75. Also it seems to be preferable to make the measurements in the mid-afternoon. Figure 17 shows the Brussels' results. Table IV below gives some results for different receiving conditions and supports the conclusions.

The results of similar measurements made at Boulder

TABLE IV
Average Standard Deviations

	Morning (10hUT)	Afternoon (15hUT)
$A_r = 0.5$	120 μ s	90 μ s
$A_r = 0.8$	70 μ s	38 μ s

NOTE: The intrinsic precision of a single measurement was between 10 and 30 microseconds.

REFERENCES

- [1] Blair, B. E., E. L. Crow and A. H. Morgan, Five years of VLF worldwide comparison of atomic frequency standards, *Radio Science*, 2, 627 (1967).
- [2] Pierce, J. S., Intercontinental frequency comparison by very low frequency radio transmission, *Proc. IRE*, 45, 795 (1957).
- [3] De Prins, J., J.-L. Guisset, J.-C. Liévin et J. Tamine, Description du système garde-temps du laboratoire d'étalons de fréquence de l'Université Libre de Bruxelles — *Annales françaises de Chronométrie*. 33e année, tome XIX.
- [4] Doherty, R. H., G. Hefley, R. F. Linfield, Timing potentials of Loran-C, *Proc. IRE*, 49, No. 11, 1659 (1961).
- [5] U. S. Coast Guard Electronics Engineering Report No. L-33, Calibration of the east coast Loran-C system.
- [6] Davis, T. L., R. H. Doherty, Widely separated clocks with

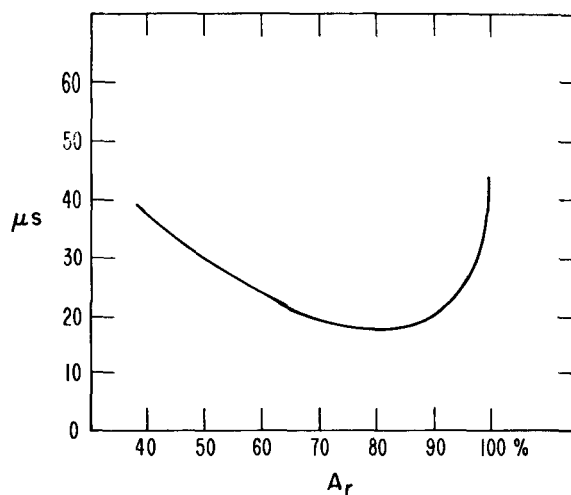


Figure 16. — Total error. $\sigma_Q = 0.05$; $\sigma_{\text{measured}} = 0.01$; $\sigma_{\text{sky-wave}} = 0.40$.

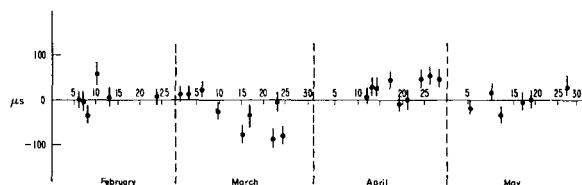


Figure 17. — Deviation of arrival times of HBC time signals as measured in the afternoon. Measurement point $A_r = 0.8$.

show a standard deviation of ± 20 microseconds. This improved accuracy was principally due to a low noise level.

We then conclude that it is possible, by taking a few simple precautions, to measure the arrival time of a low frequency pulse to a precision of ± 40 microseconds or better.

Since synchronization of the transmitters is now only within ± 25 microseconds these results are considered very encouraging.

Lastly, the method of envelope analysis should be an effective tool for the study of propagation at low frequencies.

microsecond synchronization and independent distribution systems, *IRE Wescon Convention Record*, 4, Part V, 3 (1960).

- [7] Morgan, A. H., Distribution of standard frequency and time signals, *Proc. IEEE*, 55, 827 (1967).
- [8] Chaslain, C., Propagation et réception de signaux horaires en basse fréquence — 1967 — *Memoire* — U.L.B.
- [9] Detrie, R., Réception de signaux horaires sur ondes kilométriques (conception du récepteur). *Bulletin de la Classe des Sciences*. 5e série — Tome LII — 1966.
- [10] Deleu J. et J. De Prins — Méthodes d'optimisation (To be published in 1968)
- [11] Miscellaneous Publication 236, 1967 Edition, U. S. Department of Commerce, NBS standard frequency & time services, Radio Stations WWV, WWVH, WWVB, WWVL, p. 8.